HHS Public Access

Author manuscript

J Photochem Photobiol B. Author manuscript; available in PMC 2016 March 09.

Published in final edited form as:

J Photochem Photobiol B. 2013 December 5; 129: 100–107. doi:10.1016/j.jphotobiol.2013.10.006.

The *agr* function and polymorphism: impact on *Staphylococcus aureus* susceptibility to photoinactivation

Mariusz Grinholc[1,#], **Joanna Nakonieczna**[1], **Alessandro Negri**[1], **Aleksandra Rapacka-Zdonczyk**[1], **Agata Motyka**[1], **Grzegorz Fila**[1], **Julianna Kurlenda**[2], **Justyna Leibner-Ciszak**[3], **Michael Otto**[4], and **Krzysztof P. Bielawski**[1]

[1]Laboratory of Molecular Diagnostics, Department of Biotechnology, Intercollegiate Faculty of Biotechnology University of Gdansk and Medical University of Gdansk, Kladki 24, 80-822 Gdansk, Poland [2]The State Higher Vocational School in Koszalin, Lesna 1, 75-582 Koszalin, Poland [3]BLIRT SA (BioLab Innovative Research Technologies), Trzy Lipy 3/1.38, 80-172 Gdansk, Poland [4]Laboratory of Human Bacterial Pathogenesis, National Institute of Allergy and Infectious Diseases, National Institutes of Health, Bethesda, MD, USA

Abstract

Staphylococcus aureus is an important human pathogen that causes healthcare-associated and community-acquired infections. Moreover, the growing prevalence of multiresistant strains requires the development of alternative methods to antibiotic therapy. One effective therapeutic option may be antimicrobial photodynamic inactivation (aPDI). Recently, *S. aureus* strain-dependent response to PDI was demonstrated, although the mechanism underlying this phenomenon remains unexplained. The aim of the current study was to investigate statistically relevant correlations between the functionality and polymorphisms of *agr* gene determined for 750 methicillin-susceptible and methicillin-resistant *S. aureus* strains and their responses to photodynamic inactivation using protoporphyrin IX. An *Alu*I and *Rsa*I digestion of the *agr* gene PCR product revealed existing correlations between the determined digestion profiles (designations used for the first time) and the PDI response. Moreover, the functionality of the *agr* system affected *S. aureus* susceptibility to PDI. Based on our results, we conclude that the *agr* gene may be a genetic factor affecting the strain dependent response to PDI.

Keywords

accessory gene regulator; gene polymorphism; photoinactivation; *Staphylococcus aureus*

[#]Corresponding author: Intercollegiate Faculty of Biotechnology, University of Gdansk and Medical University of Gdansk, Laboratory of Molecular Diagnostics, Department of Biotechnology, Kladki 24, 80-822 Gdansk, Poland. Tel/fax (48-58) 523 64 25. grinholc@biotech.ug.edu.pl.

Author's contribution

Conceived and designed the experiments: MG. Performed the experiments: AN, MG, AM, AR-Z, GF, JL-C. Analyzed the data: MG, JN. Contributed reagents/materials/analysis tools: MG, JK, KPB, MO. Wrote the paper: MG, JN.
All authors read and approved the final manuscript.

Competing Interest

The authors have declared that no competing interests exist.

1. Introduction

Staphylococcus aureus is one of the most important known human pathogens. It is the etiological agent in many infections, including local infections associated with skin and soft tissue damage such as wound infections, deep-seated infections (e.g., myositis or osteomyelitis), and device-related infections, as well as toxin-mediated diseases such as toxic shock syndrome (TSS) and staphylococcal foodborne diseases (SFD) [1;2]. Healthcare-associated infections, especially those caused by methicillin-resistant *S. aureus* strains (MRSA), are a great danger to both hospitalized and immunocompromised patients in whom the organism causes high morbidity and mortality [3]. *S. aureus* possesses a wide spectrum of virulence factors, including exoproteins (i.e., hemolysins, nucleases, and proteases) that facilitate host cell lysis and cell wall-associated adhesins (i.e., fibronectin-binding protein and protein A) required for the colonization of host tissues. In general, the expression of staphylococcal virulence factors is regulated through the *quorum sensing* mechanism by the accessory gene regulator (*agr*). Although the *agr* locus is conserved among staphylococcal species, it consists of a polymorphic, hypervariable fragment used to cluster *S. aureus* strains into one of four *agr* groups using polymerase chain reaction (PCR) methods [4;5].

Increasing antibiotic resistance among pathogenic bacteria has forced researchers to find alternative therapeutic options against which the bacteria will not be easily able to develop resistance. Photodynamic therapy could be one such alternative. Studies of the photoinactivation (PDI) of multiresistant pathogenic bacteria have shown that they are as susceptible to PDI as their naïve counterparts [6;7]. Photodynamic therapy (PDT), which is generally recognized as a cancer treatment, utilizes photosensitizers (PS, usually non-toxic dyes) that selectively accumulate in the target cells (i.e., malignant tissues or microorganisms; if the therapy involves microorganisms, then this therapy is termed photodynamic inactivation, or PDI) [8]. The appropriate wavelength of visible light is then used to excite the PS molecules to the singlet state, and excited sensitizers undergo triplet state reactions by either Type I or Type II pathways [9]. The Type I mechanism involves electron-transfer from the triplet state PS to the substrate, producing cytotoxic reactive species such as superoxide or hydroxyl radicals [10]. The Type II mechanism is based on energy transfer from the triplet state PS to molecular oxygen (ground triplet state) to produce highly cytotoxic singlet oxygen [11].

We have recently described the effect of PDI against different strains of *S. aureus* and demonstrated a strain-dependent effectiveness for PDI [12;13]. The mechanism underlying this phenomenon is still poorly understood. The current study is part of a wider project that aims to investigate genetic correlations with the bactericidal effect of PDI on *S. aureus*. Specifically, the aim of this study was to analyze the effect of PDI on 750 strains of both MSSA and MRSA *S. aureus* and to determine if the effect is related to different genetic profiles involving the *agr* gene. This genetic element is widely used for *S. aureus* typing and influences staphylococcal virulence. It is claimed that *agr*-group-mediated differences in the expression of various virulence factors influence strain pathogenicity and disease progression, indicating that the activity of the *agr* system affects strain virulence [5]. Thus, the search for genetic polymorphisms in this element and the determination of the genetic

background of particular strains can have an important diagnostic value. Moreover, it was shown that the *agr* system has a built-in oxidation-sensing mechanism through the DNA-binding domain of the response regulator AgrA [14]. Mutagenesis studies further established that *S. aureus* strain expressing AgrA varying in aminoacid sequence is more susceptible to H_2O_2.

Moreover, microarray analysis revealed that *agr* function is upregulated by photodynamic treatment and is related to resistance against PDI [15]. These results show that oxidation sensing is a component of the *quorum-sensing agr* signaling system and it is justified to analyse the influence of the *agr* locus, its functionality and polymorphism on *S. aureus* susceptibility to PDI which acts due to oxidative mechanisms. We hypothesise that both the functionality and polymorphism of *agr* could influence *S. aureus* susceptibility to PDI-induced oxidative mechanisms.

2. Materials and Methods

2.1. Bacterial isolates

In total, 750 clinical *S. aureus* strains isolated from 2002 to 2012 at the Provincial Hospital in Gdansk and Hospital in Koszalin, Poland, were used; of these, 307 (41.0%) were MRSA and 443 (59.0%) were MSSA. The isolates were characterized by Gram staining and the ability to produce coagulase and the clumping factor using Slidex Staph Plus (bioMèrieux, France). Species were identified using the MALDI-TOF MS (Bruker Daltonics, Germany). Methicillin resistance was determined using a disc-diffusion method as well as a latex test detecting PBP2a protein (Staphytect Plus, OXOID, US) [16]. Of the 750 strains collected, 27.5% (206 isolates) were isolated from surveillance cultures, 52.5% (394 isolates) from patients with local infections, 16.3% (122 isolates) from patients with bacteremia and generalized infections and 3.7% (28 isolates) from infections connected with endoprostheses. Additionally, the isogenic *S. aureus agr*-positive/negative pairs were used (JE2, NE95, NE1532, NE873; obtained through the Network of Antimicrobial Resistance in Staphylococcus aureus (NARSA) and *agr* isogenic pair of *S. aureus* LAC strain was used (LAC wild type, and LAC *agr*-negative mutant), and control strains of *S. aureus* listed in Table 1. Moreover, for assessment of hemolysin activity the reference *S. aureus* RN4220 was used.

2.2. MALDI-TOF MS

All strains were examined by MALDI-TOF MS using a Microflex LT instrument (Bruker Daltonics, Germany), Flexcontrol 3.0 software and the Biotyper 2.0 database (Bruker Daltonics, Germany). The data analysis was performed according to the manufacturer's instructions. The samples were covered with 1 ml matrix solution (a saturated solution of a-cyano-4-hydroxycinnamic acid in 50% acetonitrile, 2.5% trifluoroacetic acid). The analysed mass range of spectra was 2000–20 000 m/z. Each spectrum was obtained after 240 shots in an automatic acquisition mode. For the identification approach, a mass-to-charge range of 3000–15 000 Da was used. Identification was performed in duplicate and the higher score was retained. The identification score cut-off values were applied on each measurement according to the manufacturer's instructions. According to this score system, a score of < 2

is recommended for a probable species and a score of greater than 2.3 is recommended for a secure species identification [17].

2.3. Nucleic acid isolation

For DNA isolation, strains were grown overnight in nutrient trypticase soy broth (TSB) (bioMèrieux, France) at 37°C for 24 h. Then, 1.5 ml of the bacterial culture was centrifuged at 5000 x g for 10 min. The pellet was suspended in 180 μl of lysis buffer (20 mM Tris-HCl, pH 8.0, 2 mM EDTA, 1.2% Triton X-100, lysozyme 20 mg/ml) and the GeneJET™ Genomic DNA Purification Kit (Thermo Scientific, Lithuania) was used for DNA isolation according to the manufacturer's procedure. The DNA concentrations were measured using NanoDrop ND-1000 (Thermo Scientific, Lithuania) and were in the range from 10 to 100 ng per microliter. In addition, quality of the isolated DNA was confirmed by gel electrophoresis.

2.4. Random Amplification of Polymorphic DNA Fragments

To assess the clonal relatedness of studied MRSA *S. aureus* strains, the RAPD technique was applied. The isolates were typed using primer qfaseq4 – 5' CCC ACT GTG GTG TTC ATA 3'. The amplifications were performed with approximately 30–40 ng of *S. aureus* DNA in a 50 μl reaction mixture containing 5 μl of 10xTaqNova reaction buffer (750 mM Tris-HCl pH 8.8, 200 mM $(NH_4)_2SO_4$, 0.1% (v/v) Tween 20, 2 μl of 50 mM $MgCl_2$, 5 μl of dNTP mixture (2 mM of each) and 1.5 μl of primer (10 μM). This mixture was supplemented with 1 unit of TaqNova DNA polymerase (DNA-Gdansk, Poland). The PCRs were performed in a Veriti® Thermal Cycler as follows: initial denaturation at 94 °C for 2 min; ten cycles of denaturation at 94 °C for 30 s, annealing at 30 °C for 3 min and extension at 72 °C for 2 min; and 30 cycles of denaturation at 94 °C for 30 s, annealing at 50 °C for 2 min and extension at 72 °C for 2 min. After the last cycle, a final extension step was performed at 72 °C for 5 min. The amplification products were analyzed by electrophoresis of 10 μl samples on 5% polyacrylamide gels. The above RAPD protocol was established after preliminary trials of various reaction parameters (DNA, polymerase and magnesium salt concentration, PCR thermal profile optimisation) and control experiments to test the reproducibility of the method. The electrophoresis conditions were standardized and applied as follows: 10 μl of sample per well, 5% polyacrylamide gel, TBE buffer, 4.4 V/cm, 14h. The DNA bands obtained by the RAPD method described above, were visualized by UV transillumination after ethidium bromide staining. All RAPD electrophoregrams were analysed with FPQuest TM II program. The RAPD profiles were compared according to the DNA Molecular Weight Marker M10kpz (DNA-Gdansk, Poland). DNA relatedness was calculated by the band-based Dice coefficient with a setting of 2% band tolerance using the un-weighed pair group method with mathematical averaging (UPGMA). Inter-gel similarity coefficient was 90%.

2.5. *Agr* group-specific multiplex PCR

The *agr* sequences were amplified from 4 μl of the purified nucleic acid solutions in a 25 μl reaction mixture containing 1 U of *Taq* DNA Polymerase (Thermo Scientific, Lithuania), *Taq* Buffer with $(NH_4)_2SO_4$ (Thermo Scientific, Lithuania), 200 μM dNTPs (MetaBion,

Germany), 5 mM $MgCl_2$, and a 1.2 μM concentration of each of the primers Agr1-4 listed in Table 1. Amplification was performed in a BIOMETRA thermocycler (UNO II) using the following temperature program: 1 cycle of 5 min at 94°C; 30 cycles of 30 s at 94°C, 30 s at 55°C, 60 s at 72°C; and a final cycle of 7 min at 72°C. Amplification products were electrophoresed in a 1.5% agarose gel (BIORON, Germany) containing ethidium bromide and visualized by transillumination (Gel Doc 2000, Bio-Rad) under UV irradiation [18].

2.6. PCR amplification of the *agr* gene

The 1,884-bp *agr* gene fragment was amplified using primers Agr listed in Table 1. The *agr* gene was amplified from 4 μl of the purified nucleic acid solution in a 25 μl reaction mixture containing 1 U of DyNAzyme™ EXT *Taq* DNA Polymerase (Thermo Scientific, Lithuania), 10X EXT Buffer (Thermo Scientific, Lithuania), 200 μM dNTPs (MetaBion, Germany), 1.6 μM sense primer, and 1.6 μM antisense primer (Table 1). Amplification was performed in a BIOMETRA thermocycler (UNO II) using the following temperature program: 1 cycle of 4 min at 94°C; 30 cycles of 1 min at 94°C, 2 min at 55°C, 2 min at 72°C; and a final cycle of 4 min at 72°C. All samples were stored at −20°C prior to restriction enzyme digestion [19].

2.7. Restriction enzyme digestion of the PCR products

The *agr* PCR amplicons were digested with *Rsa*I (Thermo Scientific, Lithuania) and *Alu*I (Thermo Scientific, Lithuania) in a 31 μl reaction mixture containing 1 U of restriction enzyme and 10X Buffer Tango (Thermo Scientific, Lithuania). Digestions of the *agr* amplicons were performed in a BIOMETRA thermocycler (UNO II) with an incubation time of 1 h at 37°C followed by thermal inactivation of the restriction enzymes by incubation at 65°C for 20 min, according to the manufacturer's instructions. The restriction fragments were then separated by electrophoresis on a 2% agarose gel (BIORON, Germany) containing ethidium bromide and visualized by transillumination (Gel Doc 2000, Bio-Rad) under UV irradiation.

2.8. Assessment of hemolysin activity on Sheep Blood Agar plates

Cultures to be tested were grown overnight on trypticase-soy agar plates (bioMèrieux, France), cross-streaked on sheep blood agar (Biocorp, Poland) against a culture of RN4220, incubated overnight at 37°C, and then incubated for 6 h at 4°C. The patterns could be interpreted according to previously described method [20]: beta-hemolysin appears as a partially turbid zone, as seen with RN4220, which produces only beta-hemolysin. Delta-hemolysin is synergistic with beta-hemolysin and is seen as a clearing where the two hemolysins intersect. Coproduction of beta-hemolysin and delta-hemolysin is seen as a clearing next to the streak within a wider beta-hemolysin zone [20].

2.9. Photosensitizer

Protoporphyrin IX (PPIX) (MP Biomedicals, LLC, USA) was used as a sensitizer. PPIX was dissolved in dimethyl sulfoxide (DMSO; Sigma, Germany) to make a 1 mM stock solution and was stored in the dark at −20°C until use. The concentration of the photosensitizer was determined spectrophotometrically (extinction coefficient 1.6 x 10^5 M^{-1} cm^{-1}, wavelength 408 nm).

2.10. Light source

Illumination was performed using a Q.Light® PDT Lamp (b & p® Shweiz AG, Switzerland) (ISO 9001 & EN 46001 - CE 1275) (power of lamp 80 mW; fluence rate 102 mW/cm^2; fluence 6.12 J/cm^2 per minute). The delivered light energy was determined with the use of light power meter (model LM1, CARL ZEISS, Germany). The Q.Light® PDT Lamp emits polarized light (polarization level: 98%) over a wavelength range of 620 to 780 nm.

2.11. PDI studies

All bacterial isolates were subjected to photodynamic inactivation (PDI). Bacterial cultures were grown for 24 h at 37°C in nutrient trypticase soy broth (bioMèrieux, France) and then diluted with fresh broth to an appropriate density (10^7/ml bacterial cells) based on densitometry (Densi Meter II, EMO). Diluted *S. aureus* cultures were incubated with 25 μM protoporphyrin IX in the dark at 37°C for 30 min (final DMSO concentration in the sample was 2.5%). The cells were then transferred to a 96-well microtiter plate (100 μl per well) and illuminated with appropriate light (50 J/cm^2) at room temperature for 8 min and 10 s. Following illumination, 10 μl aliquots were used to determine the colony forming units (CFU). The contents of the wells were mixed before sampling, and the aliquots were serially diluted 10-fold in PBS (0.13 mM NaCl, 8.1 mM Na_2HPO_4, 2.68 mM KCl, 1.47 mM KH_2PO_4) to achieve final dilutions of 10^{-1} to 10^{-4}, which were then streaked horizontally onto square trypticase soy agar plates [21]. The plates were incubated at 37°C overnight. Controls consisted of untreated bacteria (no photosensitizers or light) kept in 96-well plates for the duration of the illumination. After 18 h of incubation at 37°C in the dark, CFUs were counted and the results were statistically analyzed. Survival fractions were expressed as ratios of CFUs of treated bacteria (with light and photosensitizer) to CFUs of untreated bacteria. The experiment was performed three times.

2.12. Statistical analysis

The statistical analyses have been performed using the statistical suite StatSoft. Inc. (2011). STATISTICA (data analysis software system). version 10.0. www.statsoft.com and Excel. The quantitive variables were characterized by the arithmetic mean of standard deviation or median or max/min (range) and 95% confidence interval. The qualitative variables were presented with the use of count and percentage. In order to check if a quantitive variable derives from a population of normal distribution, the W Shapiro-Wilk test has been used. Whereas to prove the hypotheses on homogeneity of variances, Leven (Brown-Forsythe) test has been utilized. Statistical significance of differences between two groups (unpaired variables model) was processed with the t-Student test (or Welch test in the case of lack of homogeneity) or U Mann-Withney test (in cases where conditions of performing the t-Student test were not satisfied or for variables measured by ordinal scale). The significance of difference between more than two groups were assessed with F test (ANOVA) or Kruskal-Wallis (if ANOVA conditions were not fulfilled). In the case of statistically significant differences between two groups post hoc tests were utilized (Tukey test for F or Dunn for Kruskal-Wallis). Chi-squared tests for independence were used for qualitative variables (with the use of Yates correction for cell counts below 10, with check of

Cochrane's conditions or with Fisher's exact test respectively). In all the calculations the statistical significance level of $p < 0.05$ has been used.

3. Results

3.1. Clinical isolates of *S. aureus* heterogeneously respond to PDI

All 750 strains, including both methicillin-susceptible and methicillin-resistant *S. aureus*, were subjected to photodynamic inactivation. The different strains expressed a heterogeneous response to photoinactivation, ranging from 0 to 5.1 $\log_{10}$-unit reductions in viable counts under the same experimental conditions. Among the MRSA strains, the viable count reduction ranged from 0 to 4.5 $\log_{10}$-units, while for the MSSA strains, the range was from 0 to 5.1 $\log_{10}$-units. Using the observed differences in strain responses to PDI to simplify the analysis, the strains were classified into three groups of PDI responses according to the extent of the $\log_{10}$-unit reduction in viable counts.

Terms and the ranges used for classification are shown in Table 2. The cut-offs for the categorization of PDI response was made according to lethal or sub-lethal damage caused for *S. aureus* strains. Lethal and sub-lethal conditions are defined as conditions where the direct damage is sufficient or insufficient to destroy the majority of the bacterial population [22]. Thus, lethal and sub-lethal damage were defined as resulted in > 2 $\log_{10}$ and 0–0.99 $\log_{10}$ unit reduction in viable count, respectively. Thus, strains reaching lethal or sub-lethal damage were assigned as sensitive or resistant to PDI, respectively. Strains revealing reduction in viable counts ranged between lethal and sub- lethal damage were assigned as intermediate sensitive.

The PDI effect on the 750 analyzed strains of methicillin-susceptible and methicillin-resistant *S. aureus* showed different distribution of PDI-responders across *S. aureus* population (Table 2).

3.2. Functionality of *agr* locus influences response to PDI

To establish whether *agr* gene status could correlate with PDI phenotype, the *agr* functionality test (delta-toxin hemolytic activity) was applied for all tested *S. aureus* strains. For 633 strains *agr* gene was determined to be active, as delta-toxin hemolytic activity was reported. Next, *S. aureus* groups differentiated due to the functionality of *agr* locus were compared according to their response to photodynamic treatment. Strains lacking functional *agr* system revealed increased susceptibility to PDI ($p < 0.01$) (Fig. 1). Moreover, to indicate the correlation between *agr* function and the response to PDI, the photoinactivation was applied to isogenic pairs of *S. aureus* that differ in *agr* status (*agr*-positive JE2 and *agrA*-, *agrB*- and *agrC*-negative strains, NE1532, NE95, NE873, respectively). The significant difference ($p < 0.05$) in response to PDI was observed for reference strains according to *agr* status indicating its influence on strains susceptibility to photoinactivation (Fig. 2, upper panel). When entire gene was deleted (in the case of *S. aureus* LAC isogenic strains) the difference in response to PDI was even more pronounced ($p < 0.001$) indicating the significant role of *agr* locus in *S. aureus* response to photoinactivation (Fig. 2, lower panel).

3.3. The genetic polymorphism pattern of the *agr* gene correlates with PDI phenotype

Next, to assess whether not only the functionality of *agr* locus but also its polymorphism could influences the susceptibility to PDI, 633 isolates with active *agr* gene were used for analysis of *agr* polymorphism. Thus, further analysis concerning *agr* grouping and polymorphism were performed. An *agr* group-specific multiplex PCR reaction was performed for all 633 *S. aureus* strains to amplify the *agr* sequence. The banding patterns obtained were compared to the PCR products of *agr* group-specific reference strains to determine the *agr* group for all analyzed strains. The results showed that there were statistically significant differences between *agr* groups according to the response to PDI. Strains with *agr* group 3 differently responded to photoinactivation in comparison to strains *agr* 1, 2 and 4 ($p = 0.0001$; 0.0001 and 0.0481, respectively). *Agr* group 1 strains revealed significant difference in response to PDI when compared to *agr* group 2 strains ($p = 0.001$) (Fig. 3).

To examine the genetic elements in more detail, we used PCR to amplify the *agr* gene. The PCR products were then enzymatically digested with *Alu*I, creating different digestion products that corresponded to discrete polymorphisms in the *agr* gene; these polymorphisms were subsequently named with roman numerals: I, II, IV, IVB, V, VI, VII, IX, and X (Supplementary Figure 1). Statistical analysis demonstrated that *S. aureus* strains with *Alu*I patterns II and V differently respond to PDI in comparison to patterns I, IV and IVB (significant correlations and *p* values are presented in Table 3). Interestingly, the majority of strains characterized with patterns no. I, IV, IVB, IX and X were resistant to photoinactivation (Table 3).

PCR amplicons of the *agr* gene were also subjected to *Rsa*I-based polymorphism analysis. Based on *Rsa*I restriction enzyme digestion, different digestion patterns were obtained, allowing for the classification of the analyzed strains into classes (I, II, IIB, III, IV, IVB, IVD, V, VII, and IX). Different strains express different small polymorphisms within the *agr* gene, and this determines the different restriction products (Supplementary Figure 2). Statistical analysis demonstrated that the *S. aureus* strains revealing *Rsa*I restriction pattern V respond significantly different to PDI than strains with patterns no. I, IB and IVB. Furthermore, the statistically relevant difference was reported between strains characterized with patterns II, IVB and VII (significant correlations and *p* values are presented in Table 3). Interestingly, the majority of strains revealing *Rsa*I patterns I, IB III, IV, IVB, IVD and IX represented strains resistant to photoinactivation (Table 3).

To explore the genetic characterization of the examined strains further, we applied statistical analysis to the combined *Alu*I/*Rsa*I patterns with respect to the response to PDI. This combination produced 62 divergent groups and allowed for the more precise determination of genetic elements potentially involved in the observed phenomenon. The results for the 633 methicillin-susceptible and methicillin-resistant *S. aureus* strains show that there were statistically significant differences ($p < 0.05$) between *Alu*I/*Rsa*I digestion patterns and responses to PDI. Specifically, we can conclude that the majority of strains expressing the polymorphisms associated with *Alu*I/*Rsa*I patterns I/I, IV/IV, IVB/IVB, IV/IVB and IV/II were generally the PDI-resistant strains. On the contrary, the V/VII pattern was associated

with intermediate sensitive strains (Table 4). These correlations involved both MRSA and MSSA strains excluding pattern IV/II which was solely associated with MRSA strains. In contrast, pattern V/VII was associated with IS PDI responders in the case of MSSA strains (Table 4). Statistical analysis demonstrated that *S. aureus* response to photoinactivation was significantly different between strains expressing various *Alu*I/*Rsa*I patterns (statistical correlations presented in Table 4).

It is noted that *agr* groups correlate with the clonal complexes [23;24]. Therefore, to examine the possibility that the correlation between *agr* groups and PDI response resulted from the difference in genetic background rather than *agr* polymorphism, the RAPD analysis was performed for all MRSA *S. aureus* strains. RAPD typing revealed 258 different electrophoretic patterns (with the similarity below 100%), consisting of 15–28 bands. Genetic similarity of 307 *S. aureus* strains was 61.6%. Statistical analysis of genetic relatedness allowed to distinguish 7 genetic groups - A to G (within min. similarity level – 70.5%). Among 307 *S. aureus* strains, 250 isolates of the group A proved to be clonally dependent. They were classified to 44 different genotypes (similarity level within genotype ≥90%) with the most predominant genotype “34” (represented by 46 isolates). The remaining isolates were classified as 57 different genotypes, each represented by one isolate. Interestingly, genotypically indistinguishable strains (similarity 100%) differed in their *agr* groups, *agr* polymorphisms and PDI-response indicating that the correlation between PDI susceptibility and *agr* did not result from genetic background.

4. Discussion

Recently we have demonstrated that a strain-dependent response to PDI by *S. aureus* exists, although the underlying mechanism remains unexplained [12;13]. Also Miyabe et al. tested the susceptibility of 20 *Staphylococcus* strains isolated from the human oral cavity to methylene blue mediated PACT. They demonstrated that various $\log_{10}$ units reduction could be achieved in *in vitro* tests [25]. Next, studies by Yow et al. suggested that the MRSA isolate might be more sensitive to cationic PS than *S. aureus* ATCC 25923 strains [26]. Studies by Ribeiro et al. also indicated that PDI effect is rather strain- and isolate-dependent than species-dependent [27]. One reason for the poor response to PDI could be an effective antioxidant defense system in the bacteria. *S. aureus* strains lacking active superoxide dismutases were significantly more susceptible to PPIX-based photo-killing than their native counterparts [28]. The same observation was true for a strain deprived of staphyloxanthin, a staphylococcal golden pigment known for its antioxidant properties (Nakonieczna J., unpublished results). PDI resistant phenotypes could also result from variations in biofilm production. The effect of extracellular slime on photodynamic inactivation of bacteria was also analyzed by another group, who reported that extracellular slime significantly influenced the sensitizer uptake by the *S. aureus* cells [29]. On the basis of these observations, the current study aimed to investigate statistically relevant correlations between the genetic profiles of methicillin-susceptible and methicillin-resistant *S. aureus* strains and their response to photodynamic inactivation.

Our investigation proceeded to a genetic element on the assumption that the effectiveness of photoinactivation may be related to some aspect of strain virulence. As the response to PDI

is a multifactorial phenomenon, we conducted a genetic analysis of the *agr* gene, which is the main regulator of several virulence factors that either are transported outside of the bacterial cell or are bound to the cell wall. Moreover, *agr* system revealed to be bacterial oxidation sensing system what directly combine its action with photodynamic treatment. Additionally, it was demonstrated that clinical isolates of *S. aureus* with inactive *agr* loci were also strong biofilm producers [30], indicating the impact of *agr* loci to biofilm production. Recent studies by Geisinger *et al.* (2012) demonstrated the presence of *agr* allele-dependent differences in *agr* activation. These differences were influenced by polymorphisms within the *agr* regulon that affected variations in the expression of several exoproteins and surface factors involved in pathogenesis [31]. Thus, we hypothesized that *agr* functionality and polymorphism could influence *S. aureus* susceptibility to PDI-induced oxidative mechanisms.

S. aureus strains exhibit well-defined genetic polymorphisms within the *agr* locus. Four *agr* genotypes, group I to IV, have been described to date [32]. The classification of *S. aureus* strains into four *agr* groups showed that there were statistically significant differences between the *agr* groups according to the response to PDI. Hence, our work proceeded to a more detailed analysis of the *agr* gene, focusing on *agr* gene polymorphisms. The data obtained allowed us to determine that strains expressing specific *Alu*I/*Rsa*I polymorphic patterns (listed in Table 4) were connected with strain's resistance or intermediate sensitivity to photoinactivation and that they distributed differently among MRSA and MSSA *S. aureus* strains. Based on these results, we can further hypothesize that the *agr* gene may be a genetic factor associated with strain-dependent responses to PDI, as statistically significant correlations were found between *agr* gene polymorphisms and strain responses to PDI. The *agr* locus is complex, consisting of two divergent transcription units, driven by promoters P2 and P3 (reviewed in reference [33]). The P2 operon encodes a two-component signaling module, of which AgrC is the receptor and AgrA is the response regulator. It also encodes two proteins, AgrB and -D, which combine to produce and secrete an autoinducing peptide (AIP) that is the ligand for AgrC. AgrA activates the *agr* P3 promoter, which drives the synthesis of RNAIII, the effector of target gene regulation [34]. As *agr* controls a large set of genes, including most of those encoding cell wall associated and extracellular proteins as well as biofilm formation it is hard to identify specific pathway involved in *S. aureus* susceptibility to photodynamic treatment [35]. The association between *agr* specific group, the type of infection, and also antibiotic resistance has been reported by many researchers [36]. We can assume that polymorphism within *agr* locus could impact RNAIII transcription, function, or stability what may result in various expression of related genes and/or biofilm production influencing *S. aureus* susceptibility to oxidative stress. Nevertheless, to determine underlying mechanisms further investigations must be performed i.e. RNAIII transcription profiles, or *agr* locus sequencing.

One could claim that because the isolates were obtained from one hospital, the *agr* typing could simply be clustering the isolates into particular clonal types that may be more or less susceptible to PDI and that do not influence directly the mechanism of strain-dependent responses to photoinactivation. We cannot exclude this possibility; however, if it was true, we would assume that other typing method such as RAPD analysis (current study and data

previously published by our research group, Grinholc *et al.* 2008) would also cluster the strains according to their PDI susceptibility. As only *agr* typing correlates with PDI phenotypes, we can assume that this regulon influences the strain-dependent mechanism of PDI response. However, taking into consideration all of the strains, this correlation is heterogeneous and does not show a linear trend thus demonstrating the need for a broader investigation of the *agr* gene polymorphism, and additional *agr*-dependent pathways.

Applied approach to identify *agr* polymorphism (based on RFLP analysis using two digestion enzymes) divided the isolates into 62 subgroups based on *Alu*I/*Rsa*I profile. The subgroups significantly correlated with PDI response. However, 633 isolates divided into 62 subgroups suggests that the predictive power of this method may have little value in clinical use. Thus, it is required to investigate other techniques enabling detection of gene polymorphism i.e. sequencing and searching for crucial polymorphisms determining strain susceptibility to photoinactivation.

The strain dependent susceptibility towards PDI is very large, considering that there is a 5 log range in reduction in viable count after exposure. One could concern that *agr* null mutants are only showing an approximately 1 log reduction compared to an isogenic strain carrying a functional *agr*, and that means that there is a very large unexplained variation in susceptibility/resistance towards PDI between isolates that is not related to the Agr status. Thus, it is significant to remember that the mechanism underlying strain-dependent response to PDI is multifactorial and several factors could influence strain susceptibility/resistance towards photoinactivation. Nevertheless, the current work provides proof of evidence that *agr* polymorphism and functionality influences *S. aureus* response to photodynamic treatment.

Supplementary Material

Refer to Web version on PubMed Central for supplementary material.

Acknowledgments

Funding

Isogenic pairs of *agr* mutants were obtained through the Network of Antimicrobial Resistance in Staphylococcus aureus (NARSA) program supported under NIAID/NIH Contract#HHSN272200700055C. MALDI-TOF MS analysis were performed at LM Bruss Laboratory in Poland. This work was supported by the grant no. 1651/B/P01/2010/39 from the National Science Centre (NCN). M.O. was supported by the Intramural Research Program of the National Institute of Allergy and Infectious Diseases (NIAID), U.S. National Institutes of Health (NIH).

The funders had no role in study design, data collection and analysis, decision to publish, or preparation of the manuscript.

Reference List

1. Lowy FD. Staphylococcus aureus infections. N Engl J Med. 1998; 339:520–532. [PubMed: 9709046]
2. Nastaly P, Grinholc M, Bielawski KP. Molecular characteristics of community-associated methicillin-resistant Staphylococcus aureus strains for clinical medicine. Arch Microbiol. 2010; 192:603–617. [PubMed: 20544179]

3. Kurlenda J, Grinholc M, Jasek K, Wegrzyn G. RAPD typing of methicillin-resistant Staphylococcus aureus: a 7-year experience in a Polish hospital. Med Sci Monit. 2007; 13:MT13–MT18. [PubMed: 17534242]
4. Jarraud S, Mougel C, Thioulouse J, Lina G, Meugnier H, Forey F, Nesme X, Etienne J, Vandenesch F. Relationships between Staphylococcus aureus genetic background, virulence factors, agr groups (alleles), and human disease. Infect Immun. 2002; 70:631–641. [PubMed: 11796592]
5. Traber KE, Lee E, Benson S, Corrigan R, Cantera M, Shopsin B, Novick RP. agr function in clinical Staphylococcus aureus isolates. Microbiology. 2008; 154:2265–2274. [PubMed: 18667559]
6. Wainwright M. Photodynamic antimicrobial chemotherapy (PACT). J Antimicrob Chemother. 1998; 42:13–28. [PubMed: 9700525]
7. Wilson M, Pratten J. Lethal photosensitisation of Staphylococcus aureus in vitro: effect of growth phase, serum, and pre-irradiation time. Lasers Surg Med. 1995; 16:272–276. [PubMed: 7791501]
8. Hamblin MR, Newman EL. On the mechanism of the tumour-localising effect in photodynamic therapy. J Photochem Photobiol B. 1994; 23:3–8. [PubMed: 8021748]
9. Ochsner M. Photophysical and photobiological processes in the photodynamic therapy of tumours. J Photochem Photobiol B. 1997; 39:1–18. [PubMed: 9210318]
10. Athar M, Mukhtar H, Bickers DR. Differential role of reactive oxygen intermediates in photofrin-I- and photofrin-II-mediated photoenhancement of lipid peroxidation in epidermal microsomal membranes. J Invest Dermatol. 1988; 90:652–657. [PubMed: 2834456]
11. Redmond RW, Gamlin JN. A compilation of singlet oxygen yields from biologically relevant molecules. Photochem Photobiol. 1999; 70:391–475. [PubMed: 10546544]
12. Grinholc M, Szramka B, Kurlenda J, Graczyk A, Bielawski KP. Bactericidal effect of photodynamic inactivation against methicillin-resistant and methicillin-susceptible Staphylococcus aureus is strain-dependent. J Photochem Photobiol B. 2008; 90:57–63. [PubMed: 18093839]
13. Grinholc M, Zawacka-Pankau J, Gwizdek-Wisniewska A, Bielawski KP. Evaluation of the role of the pharmacological inhibition of Staphylococcus aureus multidrug resistance pumps and the variable levels of the uptake of the sensitizer in the strain-dependent response of Staphylococcus aureus to PPArg(2)-based photodynamic inactivation. Photochem Photobiol. 2010; 86:1118–1126. [PubMed: 20630028]
14. Sun F, Liang H, Kong X, Xie S, Cho H, Deng X, Ji Q, Zhang H, Alvarez S, Hicks LM, Bae T, Luo C, Jiang H, He C. Quorum-sensing agr mediates bacterial oxidation response via an intramolecular disulfide redox switch in the response regulator AgrA. Proc Natl Acad Sci U S A. 2012; 109:9095–9100. [PubMed: 22586129]
15. Park HJ, Moon YH, Yoon HE, Park YM, Yoon JH, Bang IS. Agr function is upregulated by photodynamic therapy (PDT) for Staphylococcus aureus and is related to resistance against PDT. Microbiol Immunol. 2013; 57:547–552. [PubMed: 23668640]
16. CLSI. CLSI approved standard M100-S17. Clinical and Laboratory Standards Institute; Wayne, PA: 2007. Performance standards for antimicrobial susceptibility testing.
17. Szabados F, Woloszyn J, Richter C, Kaase M, Gatermann S. Identification of molecularly defined Staphylococcus aureus strains using matrix-assisted laser desorption/ionization time of flight mass spectrometry and the Biotyper 2.0 database. J Med Microbiol. 2010; 59:787–790. [PubMed: 20360398]
18. Lina G, Boutite F, Tristan A, Bes M, Etienne J, Vandenesch F. Bacterial competition for human nasal cavity colonization: role of Staphylococcal agr alleles. Appl Environ Microbiol. 2003; 69:18–23. [PubMed: 12513972]
19. Papakyriacou H, Vaz D, Simor A, Louie M, McGavin MJ. Molecular analysis of the accessory gene regulator (agr) locus and balance of virulence factor expression in epidemic methicillin-resistant Staphylococcus aureus. J Infect Dis. 2000; 181:990–1000. [PubMed: 10720522]
20. Ji G, Pei W, Zhang L, Qiu R, Lin J, Benito Y, Lina G, Novick RP. Staphylococcus intermedius produces a functional agr autoinducing peptide containing a cyclic lactone. J Bacteriol. 2005; 187:3139–3150. [PubMed: 15838041]
21. Jett BD, Hatter KL, Huycke MM, Gilmore MS. Simplified agar plate method for quantifying viable bacteria. Biotechniques. 1997; 23:648–650. [PubMed: 9343684]

22. Dodd CER, Sharman RL, Bloomfield SF, Booth IR, Stewart GSAB. Inimical processes: Bacterial self-destruction and sub-lethal injury. Trends Food Sci Technol. 1997; 8:238–241.
23. Monecke S, Slickers P, Ehricht R. Assignment of Staphylococcus aureus isolates to clonal complexes based on microarray analysis and pattern recognition. FEMS Immunol Med Microbiol. 2008; 53:237–251. [PubMed: 18507678]
24. Robinson DA, Monk AB, Cooper JE, Feil EJ, Enright MC. Evolutionary genetics of the accessory gene regulator (agr) locus in Staphylococcus aureus. J Bacteriol. 2005; 187:8312–8321. [PubMed: 16321935]
25. Miyabe M, Junqueira JC, Costa AC, Jorge AO, Ribeiro MS, Feist IS. Effect of photodynamic therapy on clinical isolates of Staphylococcus spp. Braz Oral Res. 2011; 25:230–234. [PubMed: 21359491]
26. Yow CM, Tang HM, Chu ES, Huang Z. Hypericin-mediated photodynamic antimicrobial effect on clinically isolated pathogens. Photochem Photobiol. 2012; 88:626–632. [PubMed: 22233203]
27. Ribeiro AP, Pavarina AC, Dovigo LN, Brunetti IL, Bagnato VS, Vergani CE, Costa CA. Phototoxic effect of curcumin on methicillin-resistant Staphylococcus aureus and L929 fibroblasts. Lasers Med Sci. 2013; 28:391–398. [PubMed: 22358772]
28. Nakonieczna J, Michta E, Rybicka M, Grinholc M, Gwizdek-Wisniewska A, Bielawski KP. Superoxide dismutase is upregulated in Staphylococcus aureus following protoporphyrin-mediated photodynamic inactivation and does not directly influence the response to photodynamic treatment. BMC Microbiol. 2010; 10:323. [PubMed: 21167031]
29. Gad F, Zahra T, Hasan T, Hamblin MR. Effects of growth phase and extracellular slime on photodynamic inactivation of gram-positive pathogenic bacteria. Antimicrob Agents Chemother. 2004; 48:2173–2178. [PubMed: 15155218]
30. Cafiso V, Bertuccio T, Santagati M, Demelio V, Spina D, Nicoletti G, Stefani S. agr–Genotyping and transcriptional analysis of biofilm-producing Staphylococcus aureus. FEMS Immunol Med Microbiol. 2007; 51:220–227. [PubMed: 17854479]
31. Geisinger E, Chen J, Novick RP. Allele-Dependent Differences in Quorum-Sensing Dynamics Result in Variant Expression of Virulence Genes in Staphylococcus aureus. J Bacteriol. 2012; 194:2854–2864. [PubMed: 22467783]
32. Ji G, Beavis R, Novick RP. Bacterial interference caused by autoinducing peptide variants. Science. 1997; 276:2027–2030. [PubMed: 9197262]
33. Novick RP, Geisinger E. Quorum sensing in staphylococci. Annu Rev Genet. 2008; 42:541–564. [PubMed: 18713030]
34. Seidl K, Chen L, Bayer AS, Hady WA, Kreiswirth BN, Xiong YQ. Relationship of agr expression and function with virulence and vancomycin treatment outcomes in experimental endocarditis due to methicillin-resistant Staphylococcus aureus. Antimicrob Agents Chemother. 2011; 55:5631–5639. [PubMed: 21968365]
35. Novick RP. Autoinduction and signal transduction in the regulation of staphylococcal virulence. Mol Microbiol. 2003; 48:1429–1449. [PubMed: 12791129]
36. Wright JS III, Traber KE, Corrigan R, Benson SA, Musser JM, Novick RP. The agr radiation: an early event in the evolution of staphylococci. J Bacteriol. 2005; 187:5585–5594. [PubMed: 16077103]

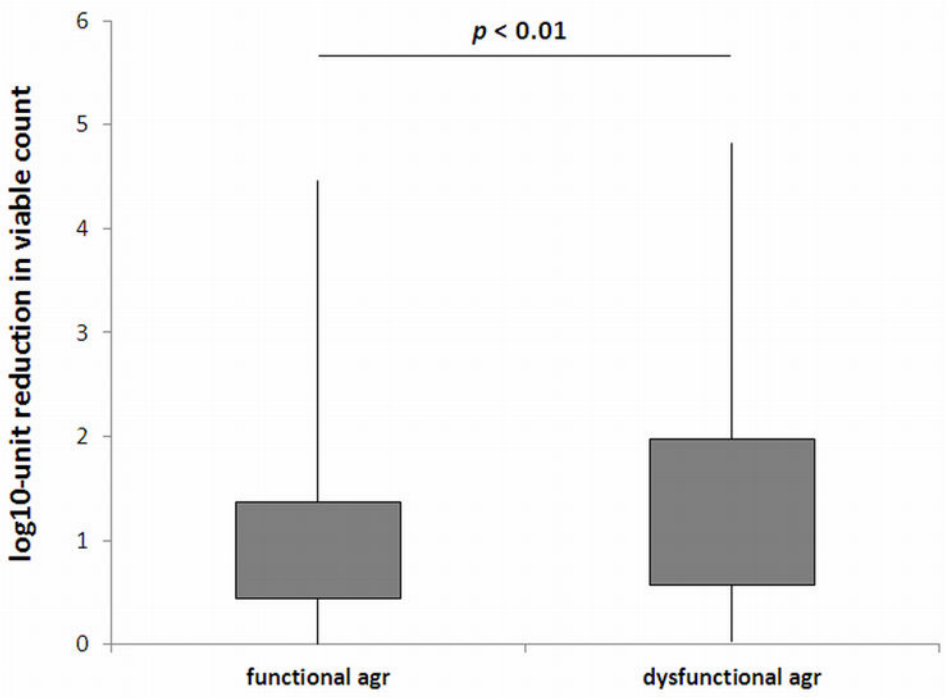

Fig. 1. Response of *S. aureus* strains differing in *agr* functionality to PPIX-mediated PDI

Each box plot represents the spread of bacterial response across the different clinical isolates. The error bars represent minimum and maximum value of $\log_{10}$-unit reduction in viable counts.

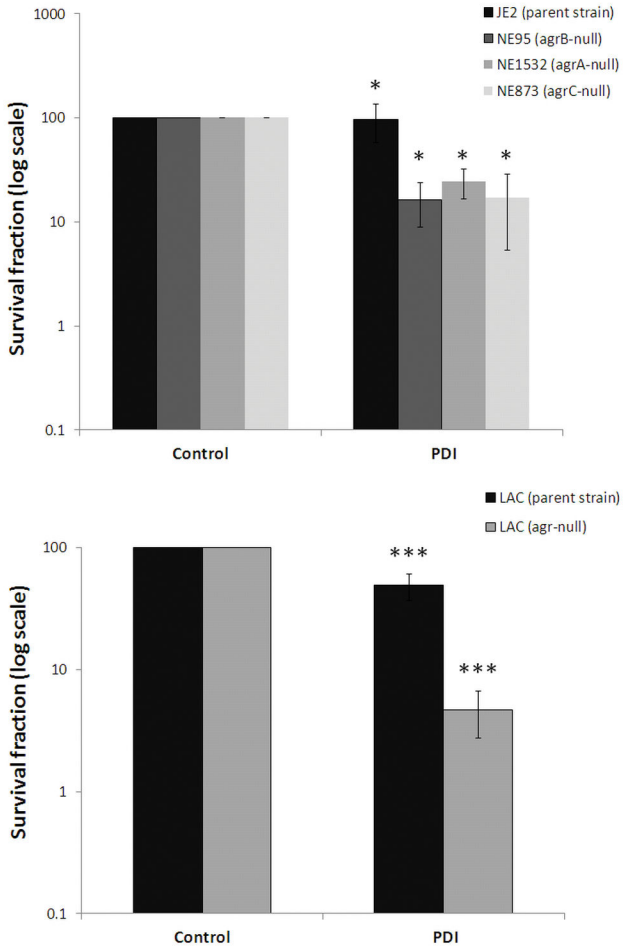

Fig. 2. Photoeffect of PPIX against isogenic *S. aureus* strains

The cells were illuminated after dark incubation for 30 min at 37°C with 25 μM PPIX with the light dose of 50 J/cm^2. The survival rate was calculated from the number of CFU in the PDI-treated sample divided by the number of CFU in the sample irradiated without photosensitizer. Each experiment was done three times, and error bars show S.D. * $p < 0.05$; *** $p < 0.001$

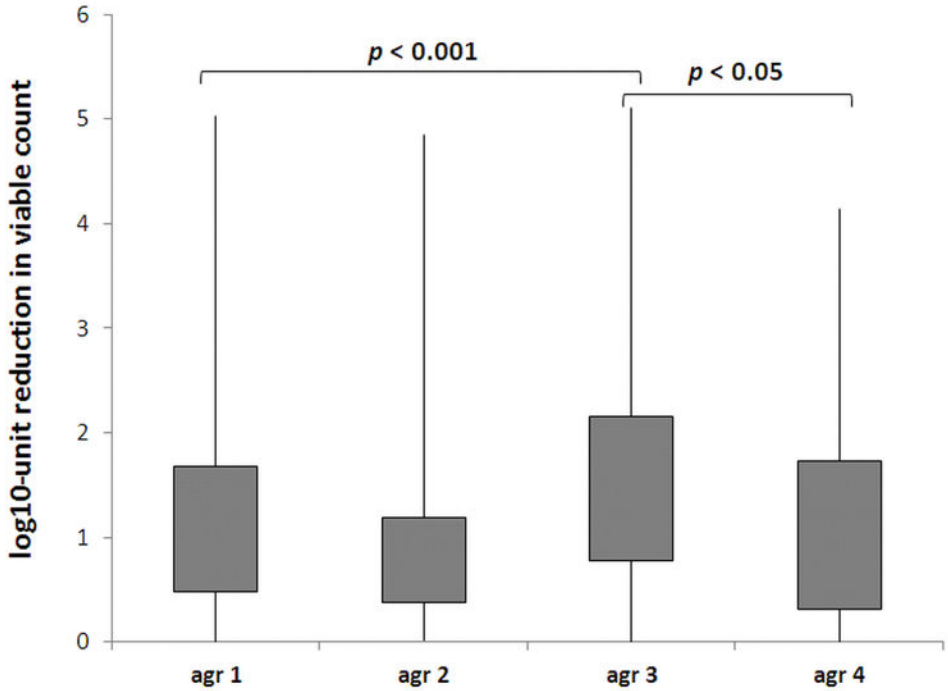

Fig. 3. Response of *S. aureus* strains differing in *agr* groups to PPIX-mediated PDI

Each box plot represents the spread of bacterial response across the different clinical isolates. The error bars represent minimum and maximum value of $\log_{10}$-unit reduction in viable counts.

Table 1

Primers and reference strains used in the study

Strain used as standard	Primer	Oligonucleotide sequence (5' – 3')	Size (bp)	Reference
RN6390	Agr	Forward: ACC AGT TTG CCA CGT ATC	1,884	[19]
		Reverse: TAA ACC ACG ACC TTC ACC		
RN6390	*Agr* 1	Forward: ATG CAC ATG GTG CAC ATG C	441	[18]
		Reverse: GTC ACA AGT ACT ATA AGC TGC GAT		
RN6607	*Agr* 2	Forward: ATG CAC ATG GTG CAC ATG C	575	[18]
		Reverse: TAT TAC TAA TTG AAA AGT GGC CAT AGC		
RN8465	*Agr* 3	Forward: ATG CAC ATG GTG CAC ATG C	323	[18]
		Reverse: GTA ATG TAA TAG CTT GTA TAA TAA TAC CCA G		
RN4850	*Agr* 4	Forward: ATG CAC ATG GTG CAC ATG C	659	[18]
		Reverse: CGA TAA TGC CGT AAT CG		

Table 2

Range of effectiveness of photosensitization

log_{10} -unit reduction	**Classification[a]**	**No. of strains (%)**
0 – 0.99	Resistant	391 (52.1)
1 – 1.99	Intermediate sensitive	210 (28.0)
2 – 5.1	Sensitive	149 (19.9)
Total		**750 (100)**

[a] Categorization made due to lethal and sub-lethal damage caused by photoinactivation

Table 3

Statistical analysis of *Alu*I and *Rsa*I determined polymorphisms over *S. aureus* response to PDI (N/%).

***Alu*I patterns**	**VI (n=46)**	**I (n=95)**	**IV (n=167)**	**IX (n=30)**	**V (n=81)**	**II (n=97)**	**X (n=12)**	**IVB (n=58)**	**VII (n=40)**
PDI categories									
R	22/47.83%	67/70.53%	103/61.68%	17/56.67%	22/27.16%	34/35.05%	7/58.33%	40/68.97%	14/35.00%
IS	13/28.26%	18/18.95%	38/22.75%	7/23.33%	32/39.51%	35/36.08%	3/25.00%	13/22.41%	16/40.00%
S	11/23.91%	10/10.53%	26/15.57%	6/20.00%	27/33.33%	28/28.87%	2/16.67%	5/8.62%	10/25.00%
Median	IS	R[1,2]	R[3,4]	R	IS[1,3,5]	IS[2,4,6]	R	R[5,6]	IS

***Rsa*I patterns**	**I (n=132)**	**IV (n=45)**	**IX (n=23)**	**V (n=50)**	**IB (n=13)**	**IVB (n=77)**	**III (n=24)**	**II (n=136)**	**IVD (n=12)**	**VII (n=68)**	**IIB (n=31)**
PDI categories											
R	84/63.64%	28/62.22%	15/65.22%	14/28.00%	11/84.62%	55/71.43%	13/54.17%	52/38.24%	8/66.67%	21/30.88%	14/45.16%
IS	28/21.21%	9/20.00%	6/26.09%	16/32.00%	2/15.38%	16/20.78%	7/29.17%	41/30.15%	3/25.00%	31/45.59%	13/41.94%
S	20/15.15%	8/17.78%	2/8.70%	20/40.00%	0/0.00%	6/7.79%	4/16.67%	43/31.62%	1/8.33%	16/23.53%	4/12.90%
Median	R[7,8]	R	R	IS[7,9,10]	R[9]	R[10,11,12]	R	IS[8,11]	R	IS[12]	IS

[1,2,3,5,10,11] $p < 0.001$

[4,6,7,8,12] $p < 0.01$

[9] $p < 0.05$ (Chi-squared test (p=0.0001), Kruskal-Wallis test (p=0.0001))

Table 4

Statistical analysis of *Alu*I/*Rsa*I patterns over *S. aureus* response to PDI (N/%).

All *S. aureus*	VI/I (n=36)	I/I (n=82)	IV/IV (n=35)	V/V (n=43)	II/II (n=68)	IVB/IVB (n=38)	VII/VII (n=37)	IV/IVB (n=38)	IV/II (n=56)	II/IIB (n=17)	V/VII (n=30)
PDI categories											
R	16/44.44%	58/70.73%	25/71.43%	11/25.58%	24/35.29%	30/78.95%	13/35.14%	24/63.16%	26/46.43%	4/23.53%	8/26.67%
IS	10/27.78%	15/18.29%	6/17.14%	13/30.23%	22/32.35%	6/15.79%	15/40.54%	10/26.32%	15/26.79%	9/52.94%	16/53.33%
S	10/27.78%	9/10.98%	4/11.43%	19/44.19%	22/32.35%	2/5.26%	9/24.32%	4/10.53%	15/26.79%	4/23.53%	6/20.00%
Median	IS	R[1,2]	R[3]	IS[1,3,4,5]	IS[2,7]	R[4,6,7]	IS	R[5]	IS	IS	IS[6]

MRSA	(n=0)	(n=66)	(n=25)	(n=22)	(n=24)	(n=32)	(n=3)	(n=28)	(n=13)	(n=4)	(n=15)
PDI categories											
R	0/0.00%	49/74.24%	19/76.00%	7/31.82%	9/37.50%	27/84.38%	0/0.00%	19/67.86%	11/84.62%	3/75.00%	7/46.67%
IS	0/0.00%	11/16.67%	5/20.00%	7/31.82%	7/29.17%	4/12.50%	3/100.00%	6/21.43%	1/7.69%	1/25.00%	7/46.67%
S	0/0.00%	6/9.09%	1/4.00%	8/36.36%	8/33.33%	1/3.13%	0/0.00%	3/10.71%	1/7.69%	0/0.00%	1/6.67%
Median	-	R[8]	R	IS[8,9]	IS[10]	R[9,10]	IS	R	R	R	IS

MSSA	(n=36)	(n=16)	(n=10)	(n=21)	(n=44)	(n=6)	(n=34)	(n=10)	(n=43)	(n=13)	(n=15)
PDI categories											
R	16/44.44%	9/56.25%	6/60.00%	4/19.05%	15/34.09%	3/50.00%	13/38.24%	5/50.00%	15/34.88%	1/7.69%	1/6.67%
IS	10/27.78%	4/25.00%	1/10.00%	6/28.57%	15/34.09%	2/33.33%	12/35.29%	4/40.00%	14/32.56%	8/61.54%	9/60.00%
S	10/27.78%	3/18.75%	3/30.00%	11/52.38%	14/31.82%	1/16.67%	9/26.47%	1/10.00%	14/32.56%	4/30.77%	5/33.33%
Median	IS	R	R	S	IS	-	IS	-	IS	IS	IS

[1,4] $p < 0.001$

[2,3,7] $p < 0.01$

[5,6,8,9,10] $p < 0.05$ (Chi-squared test (p=0.0001), Kruskal-Wallis test (p=0.0001))